An UAV for 3D Tree Surveying Method as an Improvement for Dam Construction Environmental Impact Manifestation in Mexico

Kevin D. Rodríguez González¹, Fabiola D. Yépez-Rincón ^{1*}, Jacinto Treviño Carreón², Ivone Zapata Wah¹, Adrián L. Ferriño Fierro¹, Carlos Aguilar Treviño³, Aylet Vega Aguilar¹, Roberto Huerta García¹ and Yadira Zulema Antonio Durán¹

¹Faculty of Civil Engineering, Universidad Autónoma de Nuevo León, San Nicolás de los Garza, Nuevo León, México ²Faculty of Engineering and Sciences, Universidad Autónoma de Tamaulipas, Ciudad Victoria, Tamaulipas, México ³Teeb-Con Servicios, Ingenierías y Proyectos SA de CV, Monterrey, Nuevo León, México.

Keywords: UAV; point cloud; watershed segmentation; 3D tree inventory

Abstract

In Mexico, dam construction requires a thorough Environmental Impact Manifestation (Manifestación de Impacto Ambiental, or MIA), which is a comprehensive environmental assessment report submitted to the Secretariat of the Environment and Natural Resources (SEMARNAT) for review and authorization. The MIA, however, is a formal document that outlines the potential environmental impacts of a dam project, including construction and operation. These methodologies are obsolete compared to the currently available technologies. This study tests a new procedure of 3D tree surveying of a closed-canopy woodland of different types of forests on a dam in Linares, in eastern Mexico. A DJI drone—Matrice 350 assembly—was used to collect imagery in 16 missions during the summer of 2024. A canopy height model was built from the UAV-extracted point cloud and LiDAR bare earth surface. Treetops were delineated in a variable-sized local maxima filter, and tree crowns were outlined via inverted watershed segmentation. The outputs include a tree inventory that contains thousands of trees (location, tree height, crown polygon), varying among the different types of vegetation. These new datasets give a more comprehensive approach to establish further decision making.

1. Introduction

Reservoirs are critical infrastructure systems that offer multiple socio- economics benefits such as flood control, water storage and hydroelectric energy production. However, despite these advantages, dams also entail significant environmental impacts that must be addressed to ensure long - term sustainability (Yépez-Rincón et al., 2024).

In this context, Light Detection and Ranging (LiDAR) has emerged as a valuable tool in civil and environmental engineering, particularly in the construction and maintenance of dams, as this technology provides accurate three-dimensional (3D) terrain information. Integrating LiDAR enables the construction of 3D spatial imagery information, which is key for dam terrain monitoring (Lee and Choi, 2010).

3D surveying is an innovative approach that leverages advanced technologies to create detailed three-dimensional models of trees. It is a crucial method for environmental monitoring and ecological research Guo et al. (2020). The integration of UAVs, LiDAR and photogrammetry technology has significantly enhanced the precision and efficiency of tree surveys. UAVs provide a cost-effective and flexible solution for capturing high-resolution images, which are then processed to create detailed 3D models of trees. This method is particularly useful for assessing tree competition, growth and morphological plasticity (Gatziolis et al., 2015). Wang et al. (2023) used UAV LiDAR and hyperspectral data synergy for tree species classification, or Wei and Li (2025) used for assessing the three-dimensional vegetation for carbon sinks calculations.

The integration of various geomatic devices allows for the fusion of data to create comprehensive tree models that enable the computation of tree metric variables and provide insights into tree health, growth and biomass (Balestra et al., 2023) Advanced image processing techniques, such as image enhancement and feature matching, further improve the efficiency and accuracy of 3D forest model reconstruction (Zhu et al., 2021).

The contribution of this research is as follows:

- A consistent, decisive, and stricter method for obtaining Digital Elevation Model and Digital Surface Model for flooding assessment and to create forest inventories.
- The data used belongs to new geospatial information obtained in 2024 with UAVs and Lidar sensors.
- Studies employing these techniques offer essential information for comprehensive risk management.
- The ability to identify and quantify automatically individual trees.

1.1 Background

The water supply for the population in Monterrey Metropolitan Area (5.9 million) is carried out through three dams: Rodrigo Gómez "La Boca", José López Portillo "Cerro Prieto" and Solidaridad "El Cuchillo". Aside from these reservoirs, a fourth dam has been erected to assist in the water supply for the Monterrey Metropolitan Area and the Montemorelos and Linares municipalities.

"La Libertad" dam (Figure 1) site is located at 25°0' N and 99°17' W between the Montemorelos and Linares municipalities in the Northeast of Mexico. It is operated by Water and Sewer Services of Monterrey (SADM by its acronym in Spanish) with the goal of guaranteeing the ecological flow established by the National Water Commission (CONAGUA) and to ensure water supply for human consumption and the economic activities of the population settled downstream.

The reservoir has a conservation capacity at the ordinary maximum water level (NAMO) of 221.83 million m^3 and a total capacity at the extraordinary maximum water level (NAME by its acronym in Spanish) of 307.73 million m^3 (Gobierno de Nuevo León, 2024).



Figure 1. La Libertad dam.

2. Methodology

2.1 Data collection

LIDAR data acquisition was conducted during July and August 2024 using an unmanned aerial vehicle (UAV), DJI Matrice 350 RTK equipped with a high-resolution Lidar sensor. Flights were carried out at an altitude of 100 meters over pre-defined areas, covering a total surface area of 2,000 ha. The LiDAR sensor operated at a maximum single-return point cloud rate of 240,000 points per second and was capable of recording up to five returns , providing a detailed representation of the forest ecosystem's vertical structure—particularly valuable in areas with high vegetation density (Zhang et al., 2019; Sun et al., 2022).

2.2 Point cloud classification

A preliminary classification of the point cloud was produced to help facilitate the crown segmentation process. A digital terrain model (DTM), conducted using a Cloth Simulator Filter (Zhang *et al.*, 2016), was processed to obtain bare Earth surface elevation while a digital surface model (DSM), permitted capturing features like understory vegetation and upper canopy data. To normalize the surface elevation and represent the height of the vegetation canopy, the Canopy Height Model (CHM) was calculated using Equation 1.

$$CHM = DSM - DTM, (1)$$

where CHM = Canopy Height Model DSM = Digital Surface Model DTM = Digital Terrain Model

2.3 Tree semantic segmentation

Semantic segmentation of individual tree crowns was conducted across representative samples of the vegetation types identified within the La Libertad dam's inundation zone. These vegetation types included submontane scrub, thorny submontane scrub, planted plots, and riparian vegetation. Individual treetops were identified using the Treeiso software (Xi and Hopkinson, 2022), which implements a local-to-global segmentation scheme (Figure 2). Vegetation segmentation performed CloudCompare, an opensource platform specialized in the processing and analysis of 3D point clouds. The procedure was based on the discrimination of

vegetation elements using geometric criteria, primarily the relative height above the terrain and the local point density.

The segmentation of trees was conducted through three phases, grouping the information in small clusters at first, proceeding to the determination of large segments and the identification of individual trees.

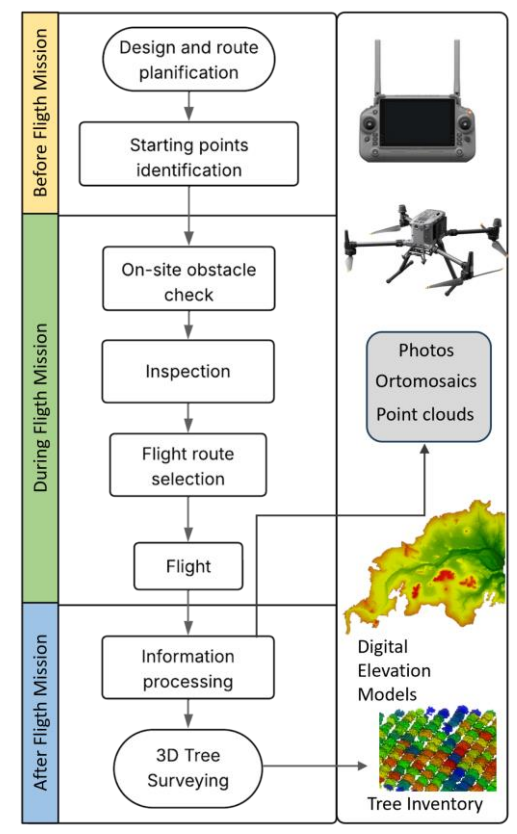


Figure 2. Methodology workflow.

2.3.1 Initial segmentation

The initial segmentation process yielded small, discrete clusters, which facilitated the identification of individual branch structures and broader crown areas. This preliminary segmentation was performed using the following parameters: a k-nearest neighbors (KNN) search with k=5 for initial cluster identification, a regularization strength of 1, and a decimated point resolution of 0.5 meters.

2.3.2 Interim segmentation

Following the initial clustering, adjacent clusters were horizontally merged using a two-dimensional cut-pursuit algorithm (Landrieu & Obozinski, 2017). The parameters employed for this merging phase were: a k-nearest neighbors (KNN) search with k=20 points, a regularization strength of 30, a maximum point gap of 2 meters, and a decimated point resolution of 0.2 meters.

2.3.3 Refined segmentation

The final stage of the segmentation process involved the merging of remaining clusters based on spatial gaps and the degree of vertical overlap, resulting in a classified point cloud of segmented individual trees. The parameters employed for this final merging phase were a vertical overlapping ratio weight of 0.5 and a relative height-to-length ratio of 0.5, utilized for the identification and separation of non-stem elements.

2.3.4 Graphics and visualization

For each vegetation type analyzed, graphical representations were generated depicting the total point count within the point cloud and the frequency distribution of points per individual tree.

2.4 NDVI

Normalized Difference Vegetation Index (NDVI) represents a fundamental tool in geomatics for evaluating spatiotemporal dynamics of vegetation cover. NDVI is one of the most widely used indices in remote sensing due to its proven capacity to estimate vegetation density and vigor based on reflectance values captured across the electromagnetic spectrum (Pettorelli et al., 2005; Tucker, 1979). The index is calculated using the following mathematical expression.

$$NDVI = \frac{(NIR - RED)}{(NIR + RED)}$$

NIR corresponds to the reflectance in the near-infrared portion of the spectrum, and RED to the reflectance in the visible red band. NDVI values range from -1 to +1. Values approaching +1 indicate dense, healthy, and photosynthetically active vegetation, whereas values near zero or negative correspond to areas with little or no vegetation cover, such as bare soil, urban surfaces, or water bodies

2.5 Orthomosaics and land use classification

The 89 generated orthomosaics were analyzed using Agisoft to calculate the Normalized Difference Vegetation Index (NDVI). This software allowed the determination of the zonal mean NDVI value for each vegetation type. Eight main classifications were identified: soil, low thorny scrub, Tamaulipas scrub, submontane scrub, riparian forest, thorny forest, and non-vegetation areas. Finally, vegetation classification maps were generated in QGIS for the entire area of the Libertad Dam, where the surface area of each vegetation type was also determined.

2.6 Botanical field survey and vegetation typing

A botanical field survey was conducted in parallel with UAV flights to support the classification and ecological interpretation of vegetation types. This work was carried out by a specialist in botany, who conducted systematic field visits across representative areas of the La Libertad dam reservoir. Species were identified in situ based on morphological characteristics and confirmed with field guides and local floristic references (Figure 3).

Each identified vegetation type (e.g., submontane scrub, thorny forest, riparian forest) was georeferenced, and dominant species

were recorded. These data provided the taxonomic foundation to validate vegetation classes derived from orthomosaics and segmentation outputs

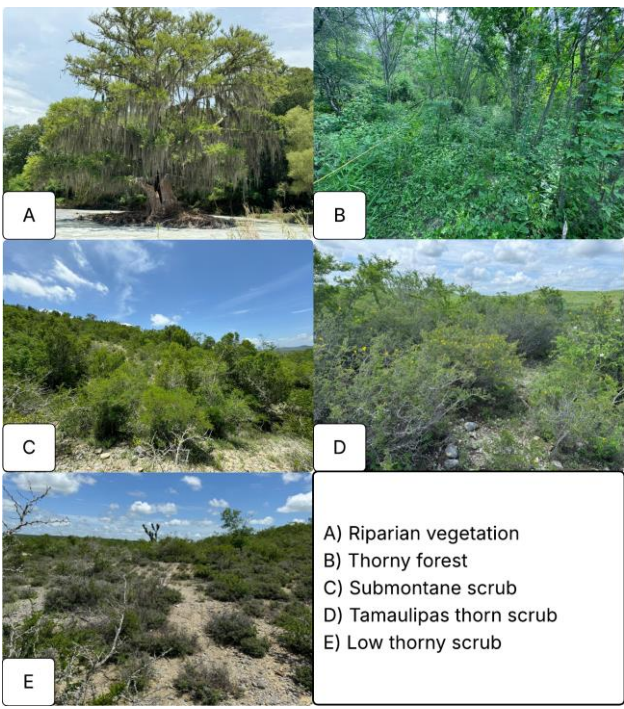


Figure 3. In-situ identified species based on morphological characteristics

3. Results

Calculating the number of trees impacted by dam construction is essential to assess environmental loss, evaluate the extent of habitat destruction for wildlife that depends on forests, estimate the release of stored carbon and its effect on climate change, plan effective reforestation or compensation strategies, understand the long-term ecological footprint of the project, comply with environmental regulations and inform sustainable development, and engage communities with transparent data for responsible decision-making.

Figure 4 illustrates the 3D structural characteristics of submontane scrub vegetation using two visualization approaches derived from the LiDAR point cloud: (a) segmentation-based rendering and (b) RGB-based rendering. In panel (a), each tree crown is assigned a different color through segmentation, enabling clear identification and delineation of individual trees, even within densely vegetated zones. Panel (b) provides a photorealistic visualization based on RGB values, which supports visual validation of the segmentation outputs (Ferraz et al., 2016). Together, these visualizations facilitate a detailed understanding of canopy structure, spatial distribution, and vegetation density, contributing to more accurate forest inventories and assessments of ecological impacts in dam-affected areas. Likewise, distinct vegetation patterns and their segmentation are identified within the Submontane Thorny Scrub ecosystem (Figure 5).

Meanwhile, the RGB visualization provides a realistic representation of canopy texture and vegetation patterns, facilitating intuitive identification of crown boundaries and spatial distribution (Wallace et al., 2012). This visual approach complements quantitative LiDAR-derived metrics and enhances

interpretation for ecological monitoring, land cover classification, and field validation.

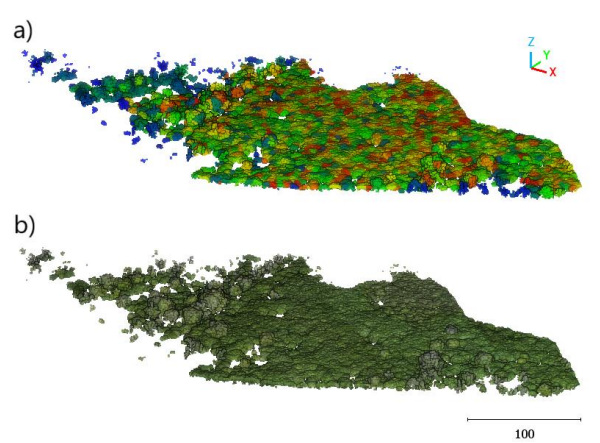


Figure 4. Submontane scrub a) Segmentation and b) RGB color.

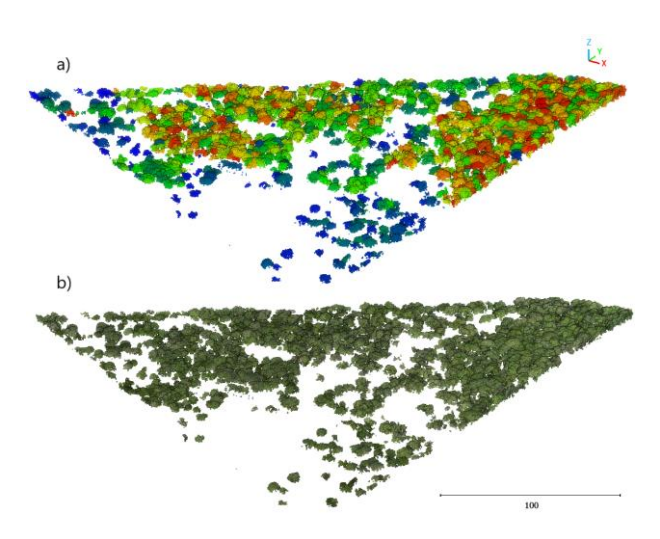


Figure 5. Submontane thorny scrub a) Segmentation and b) RGB color

This segmentation workflow was applied to the vegetation types Thorny Submontane Scrub, Crops on Plots (Figure 6), and Riparian Vegetation (Figure 7), with the aim of ensuring consistent and comparative analysis of structural parameters across all vegetation classes.

By replicating the segmentation and 3D visualization procedures for each type, detailed representations were generated that reveal differences in canopy morphology, spatial distribution, and crown architecture. This approach emphasizes structural variability and supports a more comprehensive understanding of vegetation patterns relevant to ecological impact assessments.

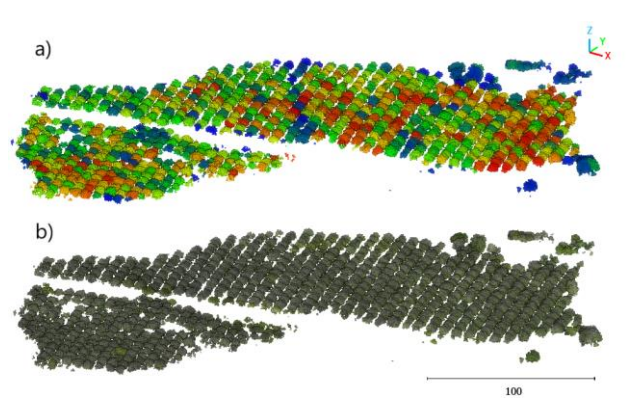


Figure. 6. Crops on plots a) Segmentation and b) RGB color

Quantifying the number of trees affected by dam construction is essential for estimating ecological damage. Metrics such as crown diameter and tree height provide valuable insights: crown size indicates the extent of canopy cover loss, while height is linked to forest maturity, carbon storage potential, and vertical habitat stratification. These parameters are critical for assessing biodiversity impacts, guiding reforestation with structurally and functionally analogous species, and ensuring accurate compensation and conservation strategies. They also support sustainable development by supplying science-based data for environmental decision-making.

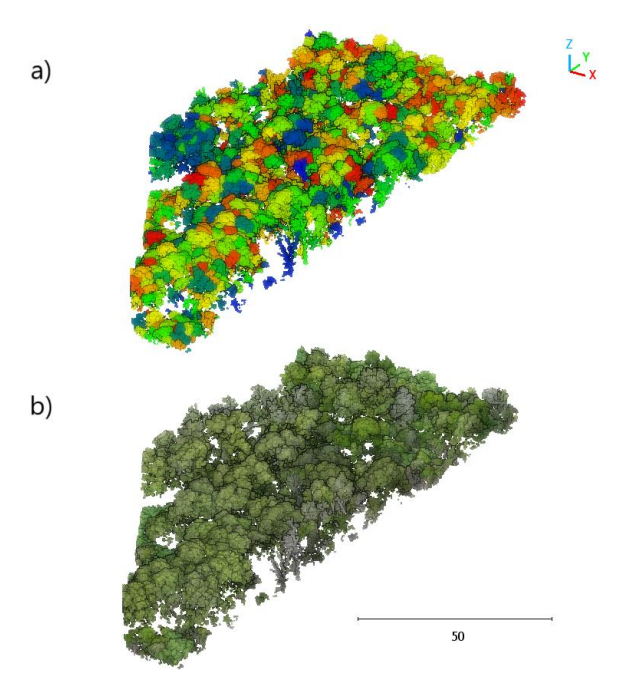


Figure 7. Riparian vegetation a) Segmentation and b) RGB color.

Results from this study show that mean crown diameters range from 3.76 m in the riparian vegetation to 6.25 m in the submontane scrub. However, these values are limited to the sampled zone within the study areas.

As shown in Table 1, submontane scrub showed the highest number of trees (n = 1774) and the largest sampling area (66,297.72 m²). This vegetation type also had the highest mean crown diameter (6.25 m) and average tree height (6.4 m), indicating a more developed forest canopy structure. In contrast, riparian vegetation (n = 1662) and thorny submontane scrub (n = 1662) and thorny submontane scrub (n = 1662) are the showest contraction of the showst contraction of the

1092) showed denser but structurally smaller canopies, while planted plots (n = 827) had moderate crown and height values, reflecting a more homogeneous and managed composition.

Vegetation type	Number of trees	Mean crown diameter (m)	Mean height (m)	Mean area (m²)	Sample area (m²)
Submontane scrub	1774	6.25	6.40	37.37	66297.72
Thorny submontane scrub	1092	5.78	5.24	29.32	32012.00
Planted plots	827	6.02	5.79	29.05	24022.31
Riparian vegetation	1662	3.76	4.00	18.92	31450.42

Table 1. Forest parameters obtained from crown segmentation in sample areas.

When normalized by sampling area, riparian vegetation showed the highest tree density, with 528 trees per hectare, due to its dense linear growth along riverbanks. In contrast, both thorny submontane scrub and planted plots had densities of 341 and 344 trees/ha, respectively. Notably, submontane scrub (Figure 8), despite having the highest number of trees overall, demonstrated the lowest density (267 trees/ha), suggesting a more heterogeneous spatial distribution and greater tree spacing.

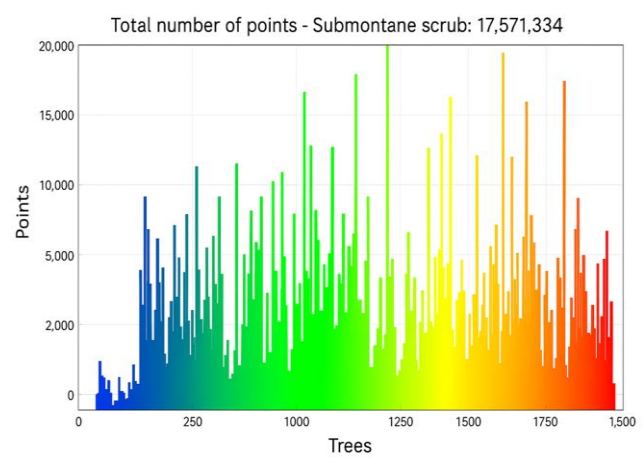


Figure 8. Submontane scrub point clouds and trees. The x-axis represents the number of trees, while the y-axis indicates the number of points associated with submontane scrub tree. Bar color gradient represents point density from low (blue) to high (red).

Conversely, the analysis of point return histograms for each vegetation type revealed distinct patterns of structural complexity and canopy organization. In the planted plots, the distribution of returns was notably uniform and compact, with most trees accumulating between 5,000 and 15,000 points. This pattern is indicative of monospecific plantations or silvicultural systems characterized by regular spacing and homogeneous canopy architecture.

In contrast, the thorny submontane scrub (Figure 9) presented a broader distribution, with individual trees reaching up to 30,000 returns, reflecting a semi-dense natural vegetation regime with moderate structural heterogeneity.

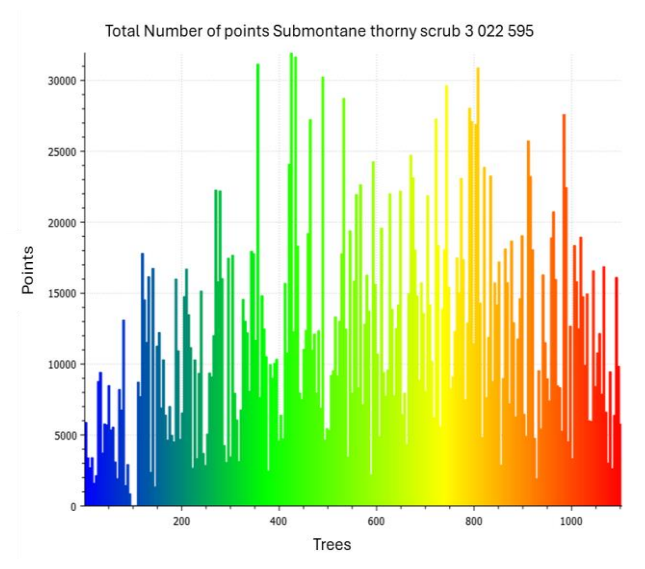


Figure 9. Submontane thorny scrub point clouds and trees. the number of submontane thorny scrub are indexed along the x-axis, while the y-axis indicates the total number of points clouds

Figure 10 presents the distribution of 3D point data across individually segmented trees within Crop plots. Each vertical bar represents the number of trees, with the number of points indicating the number of points associated with that tree in the point cloud dataset. A total of 1,882,820 points were recorded across all parcels, reflecting a high-resolution dataset likely derived from LiDAR or photogrammetric reconstruction. The bars are color-coded using a gradient from blue to red, which enhances visual differentiation across the full range of trees, although it does not correspond to a specific quantitative variable.

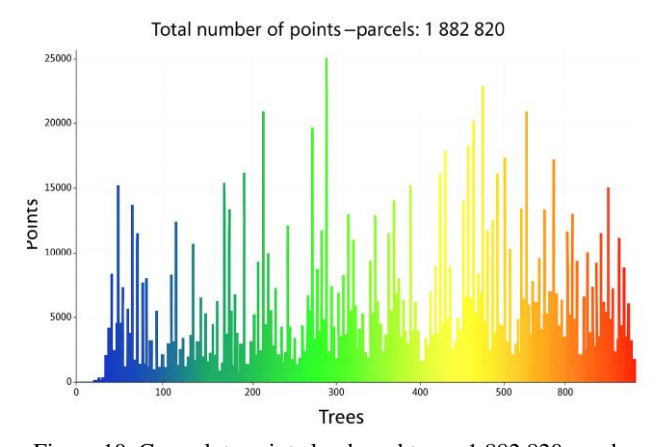


Figure 10. Crop plots point clouds and trees. 1 882 820 number of points. (Rainbow gradient applied: blue to red, representing increasing number of LiDAR points per tree)

Riparian vegetation (Figure 11) demonstrated a high return density per area, with trees often recording up to 25,000 points. This suggests densely packed, low-stature trees that typify riparian corridors, where vegetation is constrained spatially and subject to intense competition for light. The most structurally complex vegetation type was the submontane scrub, which recorded over 17 million total points, revealing large, variable crown structures and a mature forest architecture with significant vertical stratification and biomass accumulation.

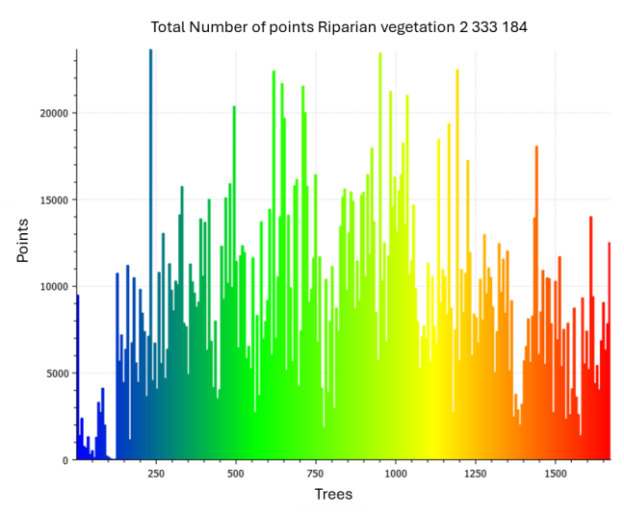


Figure 11. Riparian vegetation points clouds and trees. The x-axis represents the total number of segmented riparian vegetation trees., while the y-axis indicates the number of LiDAR points associated with each tree.

The quantity of trees for each vegetation type within the La Libertad dam's inundation zone was estimated through the extrapolation of data generated from tree crown segmentation analysis (Table 2).

Type of vegetation	Mean tree crown area (m²)	Area by type of vegetation (m ²)	Total number of trees per type of vegetation
Submontane scrubland	37.37	14 726 094.6	394 062
Thorny forest	29.32	4 577 606.8	156 126
Plots	29.05	184 506.9	6351
Riparian forest	18.92	1 764 959.4	93 285

Table 2. Distribution of trees in La Libertad Dam by vegetation type

Based on the extrapolated analysis, the estimated tree counts for each identified vegetation type within the La Libertad dam's inundation zone were as follows: submontane scrub (394,062 trees), thorny submontane scrub (156,126 trees), planted plots (6,351 trees), and riparian vegetation (93,285 trees). Furthermore, considering a 50-year flood return period, the inundation area is estimated to encompass approximately 4,459 riparian vegetation trees and 16,448 thorny submontane scrub trees.

Vegetation classification was informed not only by remote sensing analysis, but also by in-situ floristic identification conducted during field campaigns. These data were used to verify and refine the interpretation of land cover classes, ensuring ecological coherence between field and remote sensing observations. Field validation points were digitized and used to spatially correlate vegetation types observed in situ with features identified in the orthomosaics (Figure 12).

Vegetation classification was performed using high-resolution orthomosaics generated from UAV-acquired imagery over the La Libertad Dam basin. A total of 89 orthomosaics were obtained, providing detailed visual coverage of the study area for photo interpretation and post-processing NDVI.

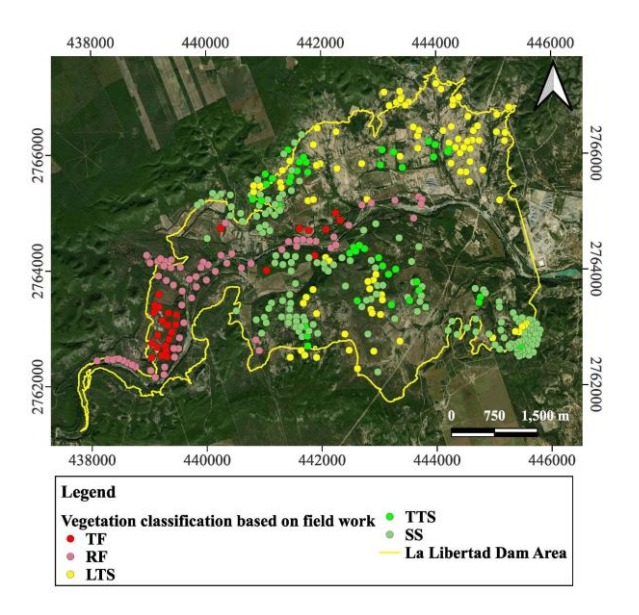


Figure 12. Vegetation classification based on field work within the La Libertad Dam area. Colored dots represent different vegetation types: TF (tropical forest), RF (riparian forest), LTS (low thorny scrub), TTS (Tamaulipas thorn scrub), and SS (submontane scrubland). The yellow outline indicates the dam area boundary.

Figure 13 illustrates the orthomosaic "Pcanal_4" with overlaid validation points corresponding to five major vegetation types: thorny forest (TF), riparian forest (RF), Tamaulipas thorn scrub (LTS and TTS), and submontane scrubland (SS). The validated orthomosaics thus served as critical inputs for enhancing classification accuracy and ecological relevance in the final vegetation mapping output.

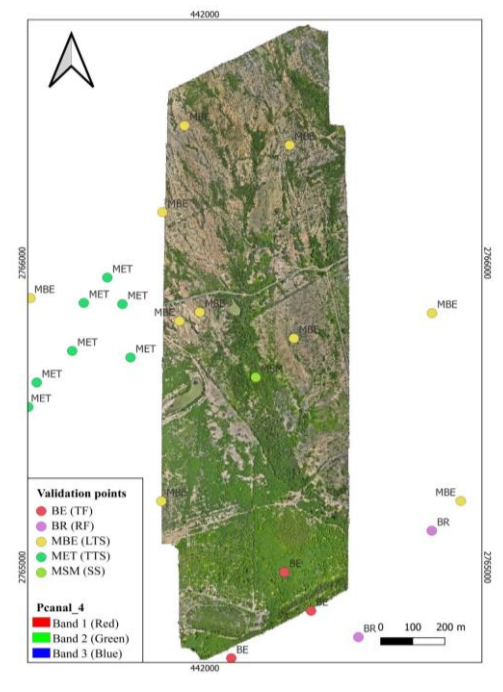


Figure 13. Orthomosaic "Pcanal_4" with validation points for the vegetation in the area of the La Libertad Dam. TF: thorny forest, RF: Riparian forest, LTS: Tamaulipas thorn scrub, TTS: Tamaulipas thorn scrub and SS: Submontane scrubland. BE. BR, MBE, MET and MSM are the acronyms in Spanish.

The 89 generated orthomosaics were analyzed for classification using NDVI. Eight main classifications were obtained: soil, low thorny scrub, Tamaulipas thorn scruaub, submontane scrubland, riparian forest, thorny forest, non-vegetal areas and field crops (Table 3).

Class	NDVI values	Vegetation type	Description		
1	0-0.05	Soil	Degraded land, soils without vegetation cover		
2	0.5-0.1	LTS (Low thorny scrub)	Scattered vegetation		
3	0.1-0.2	TTS (Tamaulipas thorn scrub)	Scattered vegetation		
4	0.2-0.4	SS (Submontane scrubland)	Open vegetation		
5	0.15-0.3	RF (Riparian forest)	Open vegetation		
6	0.15-0.25	TF (Thorny forest)	Open vegetation		
7	<0	Non-vegetal	Settlements, road infrastructure.		
8	0.15 - 0.2	Field crops	Open and anthropologically ordered vegetation		

Table 3. Vegetation types: NDVI values and description.

Vegetation classification maps were generated for the entire area of the La Libertad Dam (Figure 14). The aforementioned process was carried out for all 89 orthomosaics.

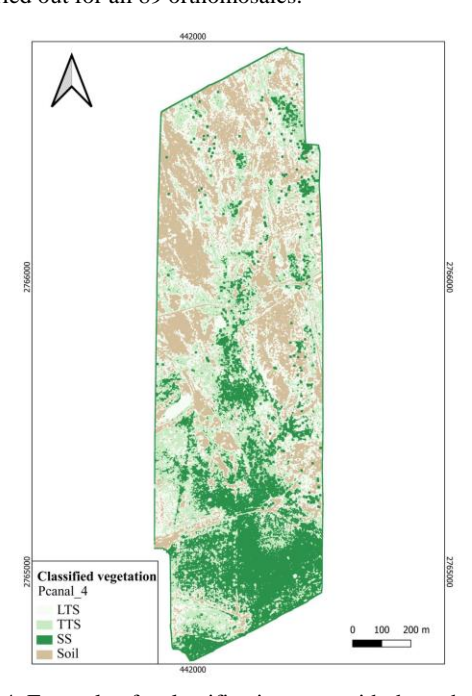


Figure 14. Example of a classification map with the orthomosaic "Pcanal_4". LTS: Low thorny scrub, TTS: Tamaulipas thorn scrub and SS: Submontane scrubland.

The NDVI values for the area of the Presa Libertad make it possible to classify vegetation and support field studies. Closed vegetation zones (riparian forest and thorn forest) are located near the river, where water runoff has favored the growth of taller and more abundant specimens. In higher areas farther from the main river, open and scattered vegetation zones are found, such as submontane scrub, Tamaulipan thorn scrub, and low thorn scrub (Figure 15). The extent of each vegetation type was calculated in square kilometers (Table 4).

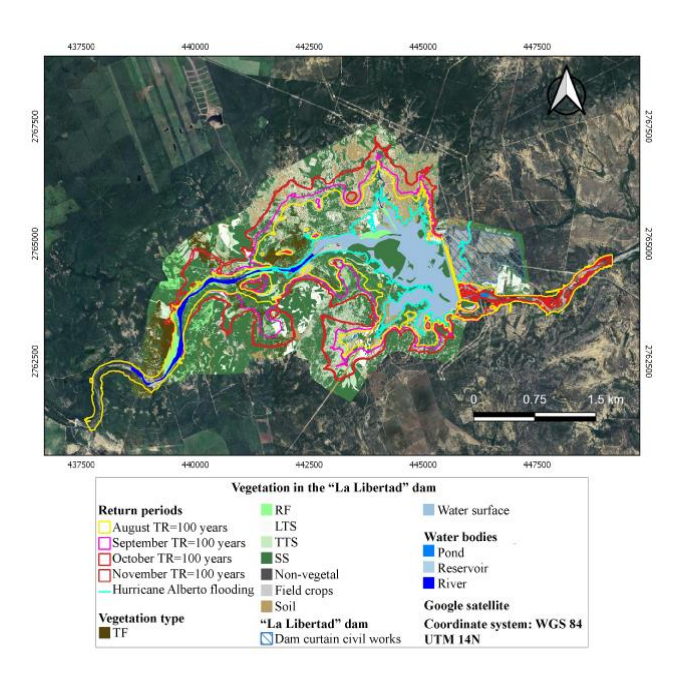


Figure 15. Vegetation in the La Libertad Dam area. Includes vegetation type classification, return periods, and flooding caused by Hurricane Alberto.

The orthomosaics show a flooded vegetated area and the varying impacts depending on the return period. The texture of the orthomosaics, together with NDVI values, made it possible to identify the riverbed, water bodies such as ponds, and the area flooded by the unexpected Tropical Storm Alberto. In addition, areas of human settlements were identified, as well as the estimation of areas corresponding to crops or plots

Total	Soil	LTS	TTS	SS	RF	TF	Non-	Field
area (km²)	(lzm²)		1	(km²)			vegetal (km²)	
5033.2		4.756		14.726		2.052	0.137	0.184

Table 4. Vegetation type areas for the entire reservoir of the La Libertad Dam.

The total vegetated area within the La Libertad dam reservoir is 27.85 km². The remaining 5.43 km² correspond to non-vegetated cover, bare soil, and agricultural plots. This means that 83.676% of the total area analyzed within the La Libertad reservoir (33.283 km²) is covered by vegetation that will be affected depending on the return periods.

4. Conclusions

This study presents a novel and replicable method for 3D tree surveying and vegetation classification in areas affected by dam construction, using UAV-based LiDAR point clouds combined with watershed segmentation algorithms. The method enabled the identification and characterization of over 650,000 trees across four main vegetation types within the La Libertad dam reservoir area. Submontane scrub showed the largest crown sizes and tree heights, while riparian vegetation exhibited the highest tree densities, reflecting structural and ecological variability across the landscape.

The integration of high-resolution point cloud data with segmentation techniques allowed for detailed quantification of

canopy structure, supporting improved environmental assessments, reforestation planning, and biomass estimation. This enhances the technical quality of Environmental Impact Manifestations (MIA) required by SEMARNAT, especially under flood risk scenarios.

Additionally, field-based botanical surveys were conducted by a specialist to identify and validate the vegetation types. A total of 143 species were recorded, spanning 122 genera and 44 botanical families, with Fabaceae being the most diverse. These in-situ identifications were used to ensure ecological consistency in the classification outputs derived from UAV imagery and segmentation results.

The study demonstrates the benefits of integrating remote sensing technologies with expert field validation to produce robust ecological inventories that inform sustainable dam development and biodiversity conservation strategies.

5. Acknowledgements

Thanks to the National Council of Humanities, Sciences and Technologies (CONAHCYT) for the scholarships of Aylet Vega Aguilar CVU: 1234261 and Kevin Rodríguez CVU:1014573, who through the Postgraduate Program of the Faculty of Civil Engineering in the Doctorate in Engineering with Orientation in Environmental Engineering at the Autonomous University of Nuevo Léon have gained the skills to partially support this type of projects, as well as the International Water Center and the Department of Geomatics, both of the Institute of Civil Engineering that provides the tools to achieve these products.

6. Funding

Financial support: This was a project supported by Servicios de Agua y Drenaje de Monterrey (SADM). Nuevo León State's water and sewage service supplier.

7. References

Balestra, M., Tonelli, E., Vitali, A., Urbinati, C., Frontoni, E., Pierdicca, R., 2023: Geomatic data fusion for 3D tree modeling: the case study of Monumental Chestnut trees. *Remote Sensing*, 15, 2197. doi.org/10.3390/rs15082197.

Ferraz, A., Saatchi, S., Mallet, C., Meyer, V., 2016: Lidar detection of individual tree size in tropical forests. *Remote Sens. Environ.*, 183, 318–333. doi.org/10.1016/j.rse.2016.05.028.

Gatziolis, D., Liénard, J., Vogs, A., Strigul, N. 2015: 3D tree dimensionality assessment using photogrammetry and small unmanned aerial vehicles. *PLoS ONE*, 10. doi.org/10.1371/journal.pone.0137765.

Guo, Q., Su, Y., Hu, T., Guan, H., Jin, S., Zhang, J., Coops, N. C., 2020: Lidar boosts 3D ecological observations and modelings: A review and perspective. *IEEE Geoscience and Remote Sensing Magazine*, 9(1), 232-257. doi.org/10.1109/MGRS.2020.3032713.

Landrieu, L., Obozinski, G. 2017: Cut pursuit: fast algorithms to learn piecewise constant functions on general weighted graphs. *SIAM J. Imaging Sci.*, 10(4), 1724-1766. doi.org/10.1137/17M1113436

Lee, G., Choi, Y., 2010: The construction of 3D spatial imagery information of dam reservoirs using LiDAR and multi beam echo sounder. *J. . Korea Spatial Information Soc.*, 18, 1-11.

Pettorelli, N., Vik, J. O., Mysterud, A., Gaillard, J. M., Tucker, C. J., Stenseth, N. C. 2005: Using the satellite-derived NDVI to assess ecological responses to environmental change. *Trends in Ecol. Evol.*, 20(9), 503–510. doi.org/10.1016/j.tree.2005.05.011

Gobierno del Estado de Nuevo León, 2024: Presa Libertad. nl.gob.mx/es/proyectos/presa-libertad (January 2025).

Sun., H., Huang, C., Zhang, H., Chen, B., An, F., Wang, L., Yun, T., 2022: Individual tree crown segmentation and crown width extraction from a heightmap derived from aerial laser scanning data using a deep learning framework. *Front. Plant Sci.*,13:914974. doi.org/10.3389/fpls.2022.914974

Tucker, C. J. 1979: Red and photographic infrared linear combinations for monitoring vegetation. *Remote Sens. of Environ.*, 8(2), 127–150. doi.org/10.1016/0034-4257

Wallace, L., Lucieer, A., Watson, C., Turner, D. 2012: Development of a UAV-LiDAR system with application to forest inventory. *Remote Sens.*, 4(6), 1519–1543. doi.org/10.3390/rs4061519

Xi, Z., Hopkinson, C. 2022: 3D graph-based individual-tree isolation (*Treeiso*) from terrestrial laser scanning point clouds. *Remote Sens.*, 14(23), 6116. doi.org/10.3390/rs14236116

Yépez-Rincón, F. D., Ferriño Fierro, A. L., Escobedo Tamez, A. N., Guerra Cobián, V. H., Pinedo Sandoval, O. E., Chávez Gómez, J. H., Pirasteh, S., 2024: Mapping longitudinal and transverse displacements of a dam crest based on the synergy of high-precision remote sensing. *Adv. Civ. Eng.*, 2024(1), 6220245. doi.org/10.1155/2024/6220245.

Zhang, W., Qi, J., Wan, P., Wang, H., Xie, D., Wang, X., Yan, G., 2016: An easy-to-use airborne LiDAR data filtering method based on cloth simulation. *Remote Sens.*, 8(6), 501. doi.org/10.3390/rs8060501

Zhu, R., Guo, Z., Zhang, X. 2021: Forest 3D reconstruction and individual tree parameter extraction combining close-range photo enhancement and feature matching. *Remote Sens.*, 13, 1633. doi.org/10.3390/rs13091633.